

A_xBA_x-Type Block–Graft Polymers with Middle Soft Segments and Outer Hard Graft Chains by Ruthenium-Catalyzed Living Radical Polymerization: Synthesis and Characterization

Yu Miura,[†] Kotaro Satoh,[†] Masami Kamigaito,^{*,†} Yoshio Okamoto,[‡] Takeshi Kaneko,[§] Hiroshi Jinnai,[§] and Syuji Kobukata[⊥]

Department of Applied Chemistry, Graduate School of Engineering, Nagoya University, Furo-cho, Chikusa-ku, Nagoya 464-8603, Japan; EcoTopia Science Institute, Nagoya University, Furo-cho, Chikusa-ku, Nagoya 464-8603, Japan; Department of Macromolecular Science and Engineering, Graduate School of Science and Engineering, Kyoto Institute of Technology, Matsugasaki, Sakyo-ku, Kyoto 606-8585, Japan; and Tsukuba Research Laboratories, Kuraray Company, Ltd., 41, Miyukigaoka, Tsukuba, Ibaraki 305-0841, Japan

Received September 9, 2006; Revised Manuscript Received November 7, 2006

ABSTRACT: Ruthenium-catalyzed living radical polymerization was applied to the synthesis of a series of all methacrylic well-defined A_xBA_x-type block–graft copolymers consisting of soft middle segments [dodecyl methacrylate (DMA)] and hard outer graft chains [methyl methacrylate (MMA)] with controlled lengths of the backbone and graft chains and controlled graft numbers. This synthetic method was based on the CHCl₂(COPh)/Ru(Ind)Cl(PPh₃)₂-initiated sequential living radical block copolymerization of DMA and 2-(trimethylsilyloxy)-ethyl methacrylate (TMSHEMA) followed by the direct transformation of the silyloxy groups into the ester with C–Br bond by 2-bromoisobutyryl bromide and the ruthenium-catalyzed “grafting-from” polymerization of MMA. A series of the block–graft copolymers were then characterized by NMR, size-exclusion chromatography (SEC), multiangle laser light scattering (MALLS), differential scanning calorimetry (DSC), dynamic viscoelasticity, transmission electron microscopy (TEM), and atomic force microscopy (AFM). The NMR and SEC-MALLS indicate the well-defined synthesis of the A_xBA_x block–graft copolymers with graft chains as branched structure. The DSC and viscoelasticity show the presence of two transitions suggesting a microphase separation, which was observed by TEM and proved different from that of the ABA triblock copolymer with the same composition. A visualization of single molecules by AFM was achieved for the first time to show the dumbbell-like structure.

Introduction

Designed polymers with well-defined architectures have been attracting much interest as new polymeric materials for many applications due to their excellent properties and various functions stemming from their unique structures, such as block, graft, and star copolymers.¹ The steady advances in living radical polymerizations over this past decade now allow the synthesis of new polymeric materials with well-defined and complex architectures,^{2–14} most of which relies on either of three processes, i.e., the nitroxide-mediated polymerization (NMP),^{2,3} the metal-catalyzed living radical polymerization or atom transfer radical polymerization (ATRP),^{4–9} and the reversible addition–fragmentation chain transfer (RAFT) polymerization.^{10,11} We have been developing the metal-catalyzed living radical polymerization of various monomers, including methacrylates, acrylates, acrylamides, styrenes, and vinyl esters, mainly based on a ruthenium or iron complex, which activates the carbon–halogen terminals via the one-electron redox reaction to reversibly generate the radical growing species.^{4,5} The ruthenium-based system was then used for the synthesis of various copolymers with precisely defined structures, such as block,^{5,15} graft,¹⁶ and star^{5,17} copolymers. We recently reported graft copolymers with controlled lengths of both the main and graft chains by the ruthenium-catalyzed living radical

“grafting-from” polymerization of methacrylates, acrylates, and styrene.¹⁶

Block and graft copolymers are generally and widely employed as compatibilizers, polymeric emulsifiers, surface modifiers, thermoplastic elastomers (TPEs), etc. Especially, the ABA-type block copolymers consisting of soft inner and hard outer chains prepared by living anionic polymerizations of dienes and styrenes and their derivatives are employed and commercialized as excellent TPEs.¹⁸ The recently developed metal-catalyzed living radical polymerizations have enabled the straightforward synthesis of fully (meth)acrylic ABA triblock copolymers consisting of a central rubbery poly(alkyl (meth)acrylate) and outer glassy poly(alkyl methacrylate),^{4,15,19,20} which can be a highly weatherable material as an alternative for the traditional styrene–diene-based TPEs. Graft copolymers are also industrially important materials, such as acrylonitrile–butadiene–styrene copolymer (ABS) and high-impact polystyrene (HIPS), which are prepared by chain-transfer reactions during conventional radical polymerizations, while well-defined graft copolymers with controlled main-chain and/or graft-chain lengths have been mostly prepared by living ionic polymerizations.¹ However, recent progresses in living radical polymerizations have also permitted not only the preparation of well-defined graft copolymers but also the modification of surfaces of base materials including films and particles.^{21–28} They provide an additional functionality to the base materials by grafting functional monomers such as hydrophilic,²⁴ hydrophobic,^{24,25} and temperature-responsive properties.^{26–28}

More complex and well-defined copolymers consisting of both block and graft structures, which are called block–graft,

[†] Department of Applied Chemistry, Nagoya University.

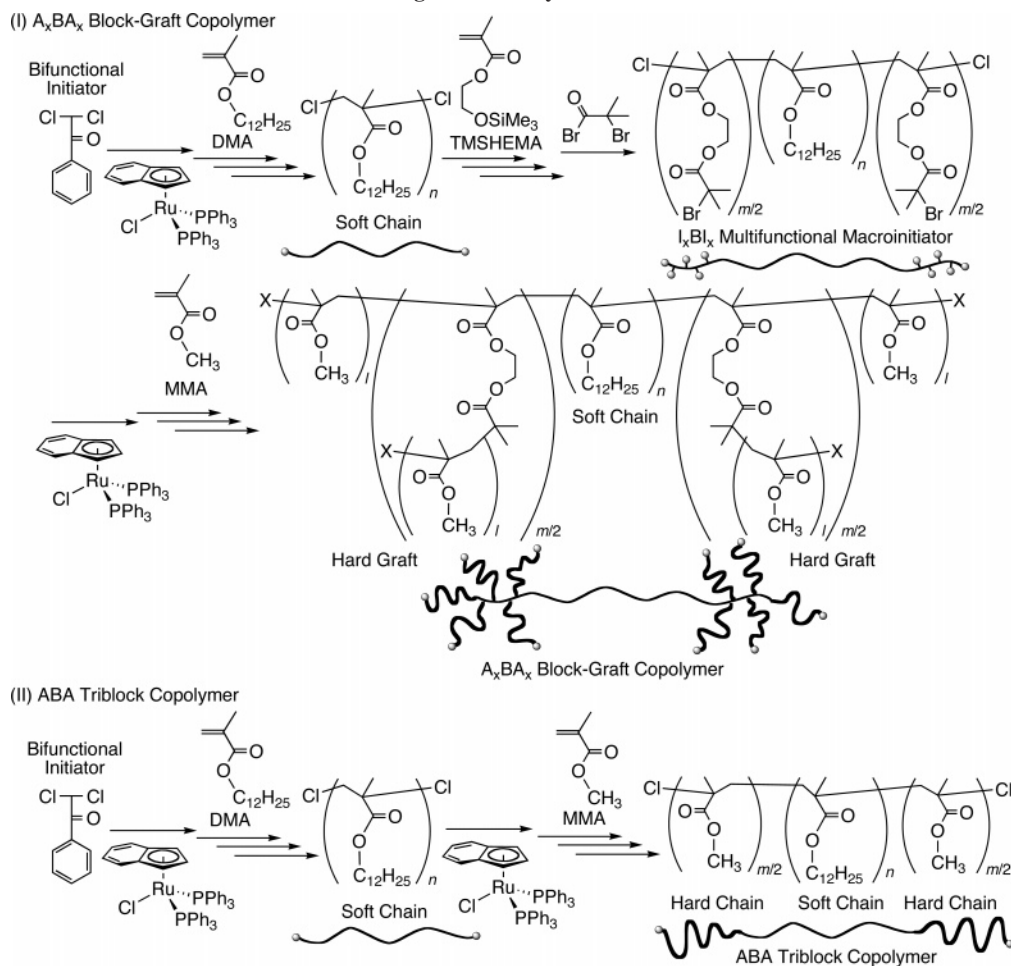
[‡] EcoTopia Science Institute, Nagoya University.

[§] Kyoto Institute of Technology.

[⊥] Kuraray Company, Ltd.

* To whom correspondence should be addressed. E-mail: kamigaito@apchem.nagoya-u.ac.jp.

Scheme 1. Synthesis of Well-Defined (I) A_xBA_x Block-Graft Copolymers and (II) ABA Triblock Copolymers via Ruthenium-Catalyzed Living Radical Polymerization



comb graft, or star block copolymers, have been attracting attention in terms of their specific architectural effects on the mechanical properties, microphase-separated morphologies, and micellization behavior.¹ Such well-structured copolymers with controlled main chain, graft chain, and block lengths have been synthesized mainly by living ionic polymerizations, except for several recent examples.^{29–42} Among them, the A_xBA_x -type block-graft copolymer, coined as dumbbell³¹ or pom-pom³² copolymers in some references, would become another type of TPE with different properties from those of the ABA triblock copolymers, when a rubbery middle segment (B) and glassy outer grafting segments (A) are employed. Although there are several reports on the synthesis of such A_xBA_x -type block-graft polymers with soft middle and hard outer graft chains, the synthesis relied on living anionic or cationic polymerization that requires cumbersome procedures including highly purifications of the reagents and fractionations of the resultant polymers in addition to the limitations of the monomers.^{33,36–39} A few of them used a combination of ionic polymerizations with the Cu-based ATRP grafting from the anionically^{37,38} or cationically³⁹ prepared ABA block copolymers with an uncontrolled number of grafting points generated via chloromethylation or bromination of the polystyrene or the poly(*p*-methylstyrene) segments, respectively. Quite recently, Ohno and Matyjaszewski reported the synthesis of an A_xAA_x -type block-graft poly(*n*-butyl acrylate) [poly(BA)], consisting of BA in the middle and outer graft chains, via Cu-catalyzed block copolymerization of BA and the poly(BA) macromonomer.⁴²

This study was thus directed to (1) the first synthesis of a series of all methacrylic A_xBA_x -type block-graft copolymers with soft middle and hard outer graft chains via the ruthenium-catalyzed living radical polymerization, (2) the characterization of the copolymers by NMR, size exclusion chromatography (SEC), multiangle laser light scattering (MALLS), differential scanning calorimetry (DSC), dynamic viscoelasticity, and transmission electron microscopy (TEM), and (3) the direct observation of the single A_xBA_x block-graft copolymer molecule by atomic force microscopy (AFM). For this, a multifunctional macroinitiator (I_xBI_x) was first prepared in one pot by the ruthenium-catalyzed living radical block copolymerization of dodecyl methacrylate (DMA) [soft middle segment (B)] and 2-(trimethylsilyloxy)ethyl methacrylate (TMSHEMA) initiated by a bifunctional initiator, followed by direct transformation of the silyloxyl group into the ester with a C-Br bond upon the reaction with 2-bromoisobutyryl bromide (I in Scheme 1). The multifunctional initiator (I_xBI_x), isolated only by precipitation, was then employed for the ruthenium-catalyzed “grafting-from” living radical polymerization of methyl methacrylate (MMA) as hard graft chains (A) to afford the A_xBA_x block-graft copolymers with the controlled length of both the backbone and the graft chains. This “grafting-from” method following the sequential living radical polymerization, and one-pot direct transformation can relatively easily enable the synthesis of a series of A_xBA_x block-graft copolymers with various backbone and graft lengths and graft numbers (n , l , and m in Scheme 1, respectively) to permit the comprehensive studies of the A_x -

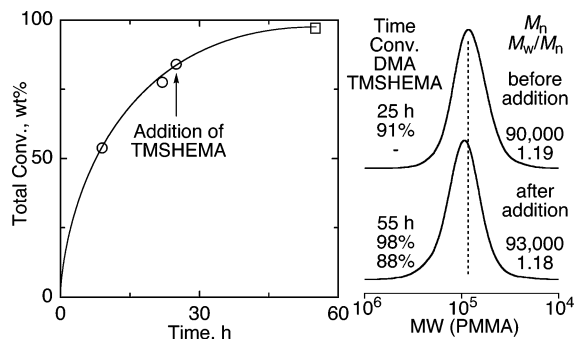


Figure 1. Ruthenium-catalyzed sequential living radical block copolymerization of dodecyl methacrylate (DMA) and 2-(trimethylsilyloxy)ethyl methacrylate (TMSHEMA) with Ru(Ind)Cl(PPh₃)₂/*n*-Bu₃N in toluene at 80 °C: before addition, [DMA]₀ = 2.5 M; [CHCl₂(COPh)]₀ = 5.0 mM; [Ru(Ind)Cl(PPh₃)₂]₀ = 0.5 mM; [*n*-Bu₃N]₀ = 10 mM (○); after addition, [TMSHEMA]_{add} = 250 mM in toluene solution (□).

BA_x block-graft copolymers. We also focused on the effects of graft structures on the microphase separation by preparing the ABA triblock copolymers of MMA and DMA (II in Scheme 1) and comparing these results. Another special note is that the dumbbell-like single molecular structure of the A_xBA_x block-graft copolymer was observed for the first time by AFM.

Results and Discussion

1. Synthesis of Multifunctional Macroinitiator: Ruthenium-Catalyzed Sequential Living Radical Block Copolymerization of DMA and TMSHEMA and One-Pot Transformation to Macroinitiator. The multifunctional macroinitiator (I_xBI_x) with soft middle poly(DMA) segments and outer multiple initiating sites was first prepared by the ruthenium-catalyzed living radical polymerization of DMA and TMSHEMA, followed by the one-pot transformation of the trimethylsilyloxy groups into the ester with a C–Br bond via direct reaction with 2-bromoisobutyryl bromide. Herein, TMSHEMA was employed as the precursor of the ester because the Ru(Ind)Cl(PPh₃)₂-catalyzed living radical polymerization gave narrower molecular weight distributions (MWDs) ($M_w/M_n \sim 1.2$) for the homopolymerization of TMSHEMA than for 2-hydroxyethyl methacrylate (HEMA).^{16,43} The use of TMSHEMA would also solve the problems in the heterogeneity of the reaction mixture during the block copolymerizations with alkyl methacrylates and HEMA. Furthermore, quantitative one-pot esterification of the TMS group with the ester bromide was possible as reported by us.¹⁶

For this, DMA was first polymerized with Ru(Ind)Cl(PPh₃)₂, which is one of most effective catalysts for the living radical polymerization of methacrylates,⁴⁴ in conjunction with 2,2-dichloroacetophenone [CHCl₂(COPh)] as the bifunctional initiator in the presence of *n*-Bu₃N in toluene at 80 °C.⁴ The ruthenium-based system was also quite effective for the methacrylate with a long alkyl chain to induce a relatively fast polymerization and to produce polymers with MWDs ($M_w/M_n \sim 1.2$), as shown in the size-exclusion chromatograms (SEC) of the produced polymers (Figure 1). After the nearly complete consumption of DMA, a feed of TMSHEMA, 10 mol % of the first DMA feed, was added to the living poly(DMA). The polymerization smoothly proceeded even after the addition of the second monomer. Figure 1 also shows the number-average molecular weights (M_n) and SEC curves of the obtained copolymer of DMA and TMSHEMA. The SEC curve shifted toward higher molecular weights retaining fairly narrow MWDs to result in the block copolymers ($M_n = 93\,000$, $M_w/M_n = 1.18$) with pendent silyloxy groups on both chain ends. Although the

prepared prepolymers were not completely block of DMA and TMSHEMA due to the addition of the second monomer before the complete consumption of the first monomer, this method relatively easily enabled the introduction of the grafting points in the both outer blocks without purification of the first polymer.

The ¹H NMR spectrum (Figure 2A) of the produced polymers showed the characteristic signals derived from DMA and TMSHEMA, i.e., the ester methylene protons (*g*) with the other alkyl protons (*h–j*) of the DMA units and the ester and silyloxy-ether methylene protons (*a* and *b*) with the trimethylsilyl groups (*c*) of the TMSHEMA units in addition to the α -methyl (*f*) and main-chain methylene protons (*e*) of both units. The unit ratio of DMA to TMSHEMA calculated from the peak intensity ratio (*a + g* vs *b*) was 490/44.1, which was in good agreement with the calculated value of 490/44.4 obtained from the feed ratio and the monomer conversions by gas chromatography. A more detailed analysis of the polymers revealed very small peaks of the aromatic protons derived from the bifunctional initiator [CHCl₂(COPh)]. The integration of the small peaks and their ratios to each monomer unit peak gave the number-average degree of polymerization of the monomer units; DP_n(DMA) = 477 and DP_n(TMSHEMA) = 46.6, which were close to the calculated values, although they may contain some experimental error originating from the very small peaks of the initiator moiety in such a high molecular weight polymer.

These results indicate that the ruthenium-based bifunctional initiating system induced the sequential living radical block copolymerization of DMA and TMSHEMA to give the triblock copolymers with controlled lengths of the soft-middle chains and the outer functional groups.

The trimethylsilyloxy groups in the triblock copolymers were then converted into the ester with a C–Br bond for the multiple “grafting-from” points via the direct reaction between the silyloxy group and the acid bromide. We have recently demonstrated that the direct transformation of the trimethylsilyl group into the ester was achievable for the random copolymers of MMA and TMSHEMA.¹⁶ Thus, 2-bromoisobutyryl bromide [Me₂C(Br)COBr] was directly added to the polymerization solution of the triblock copolymers without isolation for the one-pot transformation. The transformation was carried out with an excess amount of 2-bromoisobutyryl bromide (2.0 mol equiv to the trimethylsilyl groups) at room temperature for 24 h.

The ¹H NMR spectrum of the copolymers obtained after the reaction with Me₂C(Br)COBr exhibited typical changes (Figure 2B), in which the signal of the trimethylsilyl groups completely disappeared (*c* in Figure 2A) and peaks *a* and *b* shifted toward a lower magnetic field and changed into peaks *a'* and *b'*, respectively, along with an appearance of an additional peak attributed to the methyl groups (*d*) adjacent to the C–Br bonds. The unit ratio of DMA and the ester units (490/42.5), calculated from the peak intensity ratio (*g* vs *a' + b'*), agreed well with the ratio of DMA/TMSHEMA in the triblock prepolymer (490/44.1). The transformation efficiency based on these peak area ratios was 0.96, which also indicated the quantitative esterification. The SEC curve of the polymers also showed unimodal and narrow MWDs ($M_n = 98\,000$, $M_w/M_n = 1.16$).

These results indicate that the I_xBI_x macroinitiator was obtained by a simple one-pot reaction, i.e., the sequential living radical copolymerization of DMA and TMSHEMA followed by the in-situ transformation of the trimethylsilyl groups into the ester with the C–Br bond.

2. Synthesis of A_xBA_x Block-Graft Copolymers: Ruthenium-Catalyzed Grafting-From Polymerization of MMA. For the synthesis of the A_xBA_x block-graft copolymers with

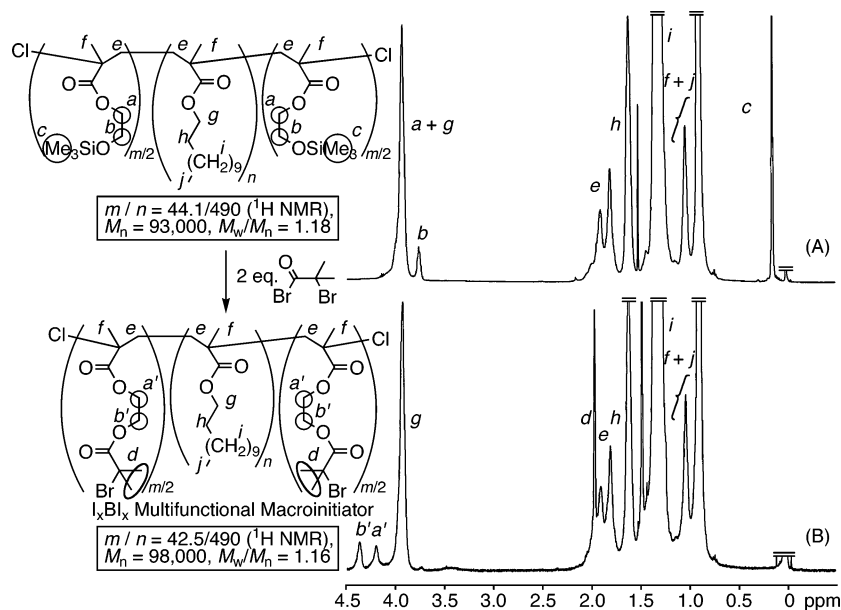


Figure 2. ¹H NMR spectra (CDCl₃, 50 °C) of the triblock copolymer of dodecyl methacrylate (DMA) and 2-(trimethylsilyloxy)ethyl methacrylate (TMSHEMA) (A; $M_n = 93\,000$, $M_w/M_n = 1.18$) and the I_xBI_x multifunctional macroinitiator obtained after the direct transformation with 2-bromoisobutyryl bromide (B; $M_n = 98\,000$, $M_w/M_n = 1.16$).

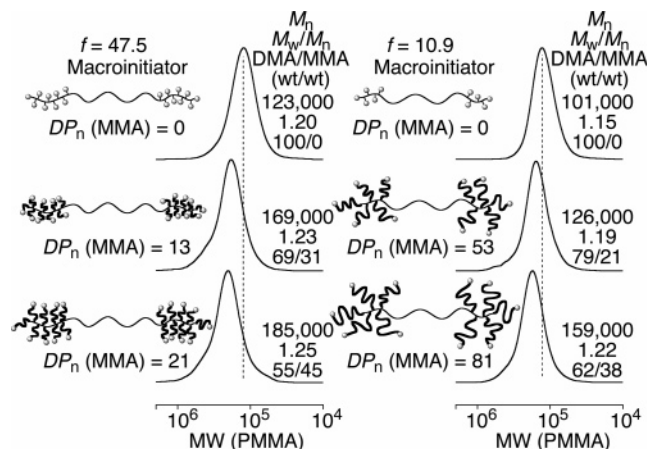


Figure 3. Graft copolymerization of methyl methacrylate (MMA) from the I_xBI_x multifunctional macroinitiator with Ru(Ind)Cl(PPh₃)₂/aluminum acetylacetonate [Al(acac)₃] in toluene at 80 °C. [MMA]₀ = 0.7 (left) or 3.0 (right) M; [C–X bonds in the macroinitiator]₀ = 9.0 (left) or 9.6 (right) mM; [Ru(Ind)Cl(PPh₃)₂]₀ = 1.0 mM; [Al(acac)₃]₀ = 40 mM.

different graft numbers, macroinitiators with different numbers of initiating sites ($f = 47.5$ and 10.9), but with the same lengths of the middle soft segments (**1** and **2**, respectively), were prepared and then employed as the multifunctional macroinitiators (Figure 3). Herein, the number of the initiating sites (f) is the sum of the number of the ester units with a C–Br bond (m in Scheme 1) and both terminal units with C–Cl bonds, i.e., $m + 2$.

The grafting polymerization of MMA from the macroinitiators was carried out with Ru(Ind)Cl(PPh₃)₂ in toluene at 80 °C in conjunction with aluminum acetylacetonate [Al(acac)₃] as an effective additive for enhancing the rate and the controllability of the ruthenium-catalyzed living radical “grafting-from” polymerization.¹⁶ The graft polymerizations smoothly proceeded to lead to the shift of the SEC curves to higher molecular weights maintaining unimodal and narrow MWDs ($M_w/M_n \sim 1.2$) for both macroinitiators. The DMA/MMA ratios calculated from the ¹H NMR spectra agreed well with the calculated values from the feed ratios and the monomer conversions.

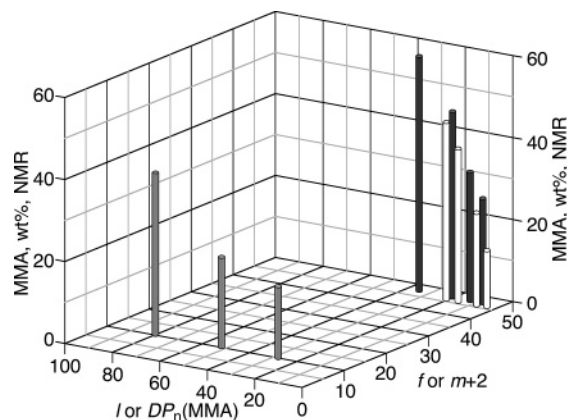


Figure 4. 3D plots of MMA contents (wt %), PMMA graft chain length [l or DP_n(MMA)], and number of initiating sites (f or $m + 2$) in the block-graft copolymers ($m \sim 500$) in the same experiment as for Figure 3.

Figure 4 is a plot of the MMA contents (wt %) obtained by the ¹H NMR spectra of the block-graft copolymers with almost the same lengths of DMA segments ($m \sim 500$) as a function of the number of initiating sites (f or $m + 2$) and the number-average degree of polymerization of the graft PMMA chains [l or DP_n(MMA)]. The MMA contents increased with the increasing f and l values and were controlled between 13% and 46% by the number (m) and the length (l) of the graft chains. This means that a series of A_xBA_x block-graft copolymers with varying MMA contents can be obtained by changing the two functions. The ruthenium-catalyzed living radical polymerization thus proved to be simple and more effective for the synthesis of a series of the A_xBA_x block-graft copolymers than the reported methods that relied on the living ionic polymerizations.^{33,36–39}

The absolute molecular weights of the A_xBA_x block-graft polymers were then measured by SEC equipped with multiangle laser light scattering (MALLS) and refractive index as a dual detector. Table 1 summarizes these data for a series of the A_xBA_x block-graft polymers with different graft numbers and graft chain lengths along with those for the ABA triblock copolymers with middle DMA and outer MMA segments.

Table 1. A_xBA_x Block-Graft and ABA Triblock Copolymers Obtained via Ruthenium-Catalyzed Living Radical Polymerization^a

code	<i>n</i> ^b	<i>f</i> ^b (<i>m</i> + 2)	<i>l</i> ^b	<i>M_n</i>		<i>M_w/M_n</i> ^d	<i>M_w</i>		<i>R_z</i> nm ^e	<i>dn/dc</i> ^f	DMA/MMA, wt/wt		<i>T_g</i> , °C ^h
				calcd ^c	SEC ^d		SEC ^d	MALLS ^e			calcd ^g	obsd ^b	
1	490	46.1	0	137 000	98 000	1.16	114 000	152 000	24.1	0.0827			n.d.
2	490	46.1	4.1	156 000	116 000	1.21	140 000	168 000	24.4	0.0989	87/13	87/13	-50.5, 54.4
3	490	46.1	8.1	174 000	126 000	1.23	155 000	190 000	24.5	0.1032	77/23	78/22	-51.8, 71.3
4	490	46.1	16	211 000	147 000	1.24	182 000	243 000	26.1	0.1123	63/37	63/37	-51.1, 86.0
5	490	46.1	21	232 000	151 000	1.23	186 000	301 000	26.8	0.1265	57/43	54/46	-52.2, 92.9
6	491	10.9	0	128 000	97 000	1.17	113 000	154 000	22.9	0.0715			n.d.
7	491	10.9	29	158 000	116 000	1.20	139 000	177 000	24.2	0.0798	80/20	84/16	-50.5, 74.4
8	491	10.9	53	184 000	126 000	1.19	150 000	225 000	28.8	0.0906	69/31	79/21	-48.5, 82.8
9	491	10.9	81	213 000	159 000	1.22	194 000	262 000	32.6	0.1201	59/41	62/38	-52.7, 97.3
10	568	2	0	145 000	116 000	1.21	140 000	178 000	25.7	0.0795			n.d.
11	568	2	182	181 000	155 000	1.21	188 000	226 000	33.2	0.0906	80/20	82/18	-52.5, 101.2
12	568	2	298	205 000	180 000	1.21	218 000	247 000	37.0	0.1011	71/29	72/28	-48.4, 116.3
13	568	2	438	230 000	199 000	1.22	243 000	273 000	46.5	0.1053	63/37	65/35	-51.2, 116.4

^a Polymerization conditions: [MMA]₀/[C-X bonds in the macroinitiator]₀/[Ru(Ind)Cl(PPh₃)₂]₀/[aluminum acetylacetonate]₀ = 700/9.0/1.0/40 mM (codes 2–5), 3000/9.6/1.0/40 mM (codes 7–9), or 4000/2.0/1.0/40 mM (codes 11–13), in toluene at 80 °C. ^b Determined by ¹H NMR. ^c *M_n*(calcd) = *M_n*(macroinitiator, calcd) + ([M]₀/[C-Br]₀) × conv × *f* × MW(MMA). ^d The number-average molecular weight (*M_n*), the weight-average molecular weight (*M_w*), and polydispersity index (*M_w/M_n*) were determined on size-exclusion chromatography (SEC) by refractive index (RI) detector (PMMA standard). ^e Measured on SEC by multiangle laser light scattering (MALLS) detector (λ = 633 nm). ^f Measured by refractometer (λ = 633 nm). ^g Calculated from feed ratio and monomer conversion. ^h Determined by differential scanning calorimetry (DSC).

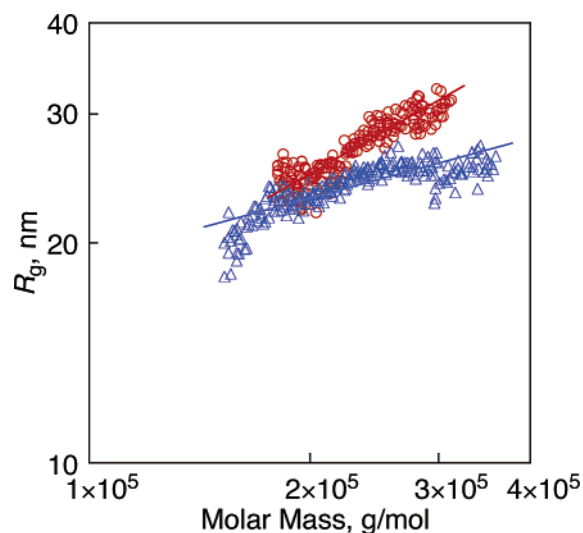


Figure 5. Double-logarithmic plots of the radius of gyration (*R_g*) and the molar mass obtained by MALLS for the ABA triblock copolymer [○; *M_n*(SEC) = 199 000, *M_w*(MALLS) = 273 000, *M_w/M_n*(SEC) = 1.22, A/B = 35/65] and the A_xBA_x block-graft copolymer [△; *M_n*(SEC) = 147 000, *M_w*(MALLS) = 243 000, *M_w/M_n*(SEC) = 1.24, A/B = 37/63, *f* = 46.1]. The solid lines indicate the fitted lines.

As shown in Table 1, the *M_w*(MALLS) was consistently higher than *M_w*(SEC) based on the standard PMMA calibration while *M_n*(SEC) was consistently lower than *M_n*(calcd). In addition, the differences between *M_w*(MALLS) and *M_w*(SEC) or between *M_n*(SEC) and *M_n*(calcd) became larger with the increasing number of graft chains (*f*). This is due to the branched structures of the block-graft copolymers. Furthermore, the *M_n* that can be calculated from *M_w*(MALLS) and *M_w/M_n* agreed well with *M_n*(calcd), which indicates the well-defined synthesis of the A_xBA_x block-graft polymers without significant coupling and chain-transfer reactions during the living radical polymerizations.

Figure 5 shows double-logarithmic plots of the radius of gyration (*R_g*) and the molecular weight obtained by MALLS for ABA triblock and A_xBA_x block-graft copolymers with almost the same molecular weights (codes 4 and 13 in Table 1). As studied earlier for linear polymers and branched or graft polymers,^{23,45} the slope of the linear plot permits linear and branched polymers to be distinguished. The typical values for linear random coils are between 0.5 and 0.6, whereas lower

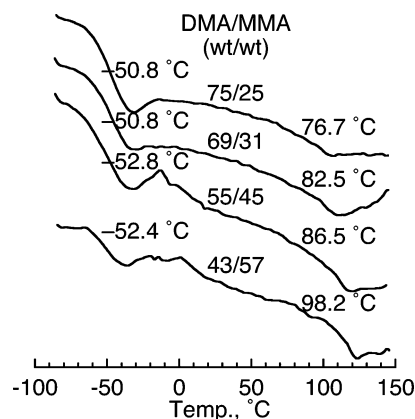


Figure 6. Differential scanning calorimetry (DSC) curves of the A_xBA_x block-graft copolymers (*f* = 47.5) obtained with the I_xBI_x multifunctional macroinitiator/Ru(Ind)Cl(PPh₃)₂/Al(acac)₃ in toluene at 80 °C.

values indicate branching. The slope for the ABA triblock copolymers (code 13) was determined to be 0.53 while that for the A_xBA_x block-graft copolymers (code 4) was 0.23. A less branched A_xBA_x copolymer (code 9) gave a slightly higher value of 0.29. These results also indicate the formation of the branched copolymers.

3. Characterization of A_xBA_x Block-Graft Copolymers.

The properties of the A_xBA_x block-graft copolymers were then characterized by various methods, such as DSC, dynamic viscoelasticity, TEM, and AFM.

Figure 6 shows the DSC curves of various A_xBA_x block-graft copolymers (DMA/MMA = 75/25–43/57, *n* = 495, *f* = 47.5, *l* = 8.1–35). For all four samples, two glass transition temperatures (*T_g*) around -50 and 75–100 °C were observed, corresponding to the transition of the rubbery poly(DMA) and glassy PMMA graft segments, respectively. The homopolymers prepared by conventional radical polymerization at 60 °C showed a *T_g* at -59 °C for poly(DMA) and at 117 °C for PMMA.⁴⁶ The presence of two glass transition temperatures indicates that the A_xBA_x block-graft copolymers have phase-separated structures.

We also analyzed all the copolymers in Table 1 by DSC. The higher transition temperature due to the PMMA graft chains increased with the increasing degree of polymerization (*l*) and reached 116.4 °C, which was almost the same as the *T_g* reported for PMMA with a similar tacticity.⁴⁶ Figure 7 is a plot of the

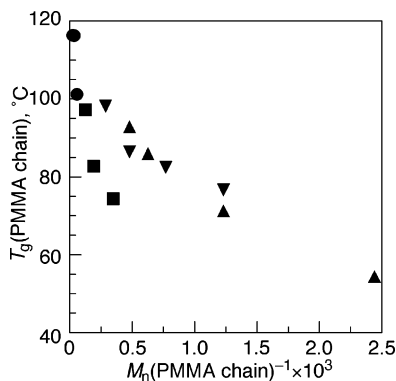


Figure 7. Plots of T_g vs $M_n(\text{PMMA chain})^{-1}$: PMMA chain of the ABA triblock copolymer (●) and $A_xB A_x$ block-graft copolymers: $f = 10.9$ (■), 46.1 (▲), and 47.5 (▼).

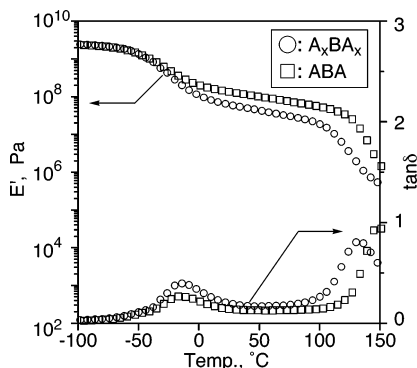


Figure 8. Dynamic tensile storage moduli (E') and $\tan \delta$ as a function of temperature for the $A_xB A_x$ block-graft copolymer (○; $M_n = 141\,000$, $M_w/M_n = 1.20$, $A/B = 32/68$, $f = 10.9$) and the ABA triblock copolymer (□; $M_n = 199\,000$, $M_w/M_n = 1.22$, $A/B = 35/65$). Heating rate: 10 °C/min; frequency: 11 Hz.

T_g values vs the reciprocal of the M_n of PMMA graft chains. In general, there is a linear relationship between T_g and $1/M_n$ for linear polymers according to Fox–Flory equation⁴⁷ while a more detailed analysis showed the presence of two lines which intersect at a critical molecular weight associated with the chain entanglements.⁴⁸ In our case, the T_g values for the ABA triblock and the $A_xB A_x$ block-graft copolymers with a lower number ($f \sim 10$) of graft chains are close to those of the linear PMMA with similar molecular weights.⁴⁸ However, the T_g s for a higher number of graft chains ($f \sim 45$) were higher than those of the linear PMMA, probably due to the cumulative effects of the graft chains connected together on the main chain.

The dynamic mechanical property of the copolymers was evaluated by the dynamic viscoelasticity. Figure 8 shows the dynamic tensile storage modulus (E') and $\tan \delta$ ($= E''/E'$) as a function of temperature for the $A_xB A_x$ block-graft copolymer (DMA/MMA = 68/32, $n = 487$, $f = 10.6$, $l = 65$) and the ABA triblock copolymer (DMA/MMA = 65/35, $n = 568$, $l = 438$). The two loss peaks in the modulus are associated with the T_g of the rubbery poly(DMA) and that of the glassy PMMA grafting chains. The modulus of the rubbery plateau of the $A_xB A_x$ block-graft copolymer was slightly lower than that of the ABA triblock copolymer, probably due to the differences in the morphologies related to the molecular structure.

The bulk morphology of the $A_xB A_x$ block-graft copolymers was thus analyzed using TEM and was compared to that of the ABA triblock copolymer. As shown in Figure 9, we analyzed three samples with almost the same DMA/MMA contents ($\sim 65/35$), but with different graft numbers and graft lengths [$A_xB A_x$: DMA/MMA = 63/37, $n = 490$, $f = 46.1$, $l = 16$ (sample a);

DMA/MMA = 68/32, $n = 487$, $f = 10.6$, $l = 65$ (sample b); ABA: DMA/MMA = 65/35, $n = 568$, $l = 438$ (sample c)]. The microphase morphology of the triblock copolymers that contain ~ 35 wt % PMMA was expected to be an assembly of cylinders or lamellae of PMMA into the matrix formed by the major component.⁴⁹ The ABA triblock copolymer sample showed a complex structure like the cocontinuous or disordered cylinders of dark PMMA domains in a brighter continuous poly(DMA) matrix (Figure 9c). A similar complex image was also observed for the (meth)acrylate-based ABA triblock copolymers of MMA and BA prepared by the living anionic block copolymerization,⁵⁰ or the difficulty in the selective staining was reported.¹⁹ These are most probably due to the similarity in the structures of these components.¹⁹ In contrast, the morphology of the $A_xB A_x$ block-graft copolymer sample was quite different for both samples. The sample with a lower graft number and longer graft chains showed a lamellae structure with long-range disorders (Figure 9b), while the sample with a higher graft number and shorter graft chains exhibited more complex lamellae-like structures (Figure 9a). Thus, the $A_xB A_x$ block-graft copolymers can form microphase-separated structures, which can be distinguished from that of the ABA triblock copolymers and largely depend on the graft numbers and lengths.

For further evaluation of the $A_xB A_x$ block-graft structure, visualization of single molecules was done by AFM for a high molecular weight polymer ($n = 495$, $f = 47.5$, $l = 247$, M_n (SEC) = 791 000, $M_w/M_n = 1.27$). Figure 10 shows the AFM micrograph of the $A_xB A_x$ block-graft copolymer cast from a 1.0 $\mu\text{g/mL}$ CHCl_3 solution on a mica plate. Several images apparently consisting of two spherical objects were observed with more than 0.3 μm distances, which suggests that each image corresponds to a single molecule. An enlarged micrograph in the inset picture shows two round-shaped images with ~ 90 nm diameters and ~ 1 nm heights, which were located at an ~ 50 nm distance. This suggested to us the dumbbell-like structure of the $A_xB A_x$ block-graft copolymer as expected. This is the first visualization of single molecules of $A_xB A_x$ block-graft copolymers while other graft copolymers with highly dense brushes prepared by Cu ATRP have been reported elsewhere.^{22,51}

Conclusions

A series of well-defined $A_xB A_x$ -type block-graft copolymers consisting of soft middle and hard outer graft chains was first prepared by a simple method based on the ruthenium-catalyzed sequential living radical block copolymerization of DMA and TMSHEMA followed by the direct transformation of the silyloxy groups into the ester with a C–Br bond and the ruthenium-catalyzed grafting-from polymerization of MMA. The DSC and dynamic viscoelastic analysis exhibited two transition points attributed to the T_g s of the poly(DMA) and PMMA segments suggesting a microphase separation, which was observed by TEM and determined to be different from that of the ABA triblock copolymers. A visualization of single molecules by AFM was achieved for the first time to show the dumbbell-like structure as expected.

Experimental Section

Materials. MMA (Tokyo Kasei, >99%) was washed with aqueous NaOH (5%) and water, dried over magnesium sulfate, and distilled from calcium hydride under reduced pressure before use. DMA (Tokyo Kasei, >99%) and TMSHEMA (Aldrich, >96%) were distilled from calcium hydride under reduced pressure before use. Ru(Ind)Cl(PPH₃)₂ (provided from Wako Chemicals) and Al-

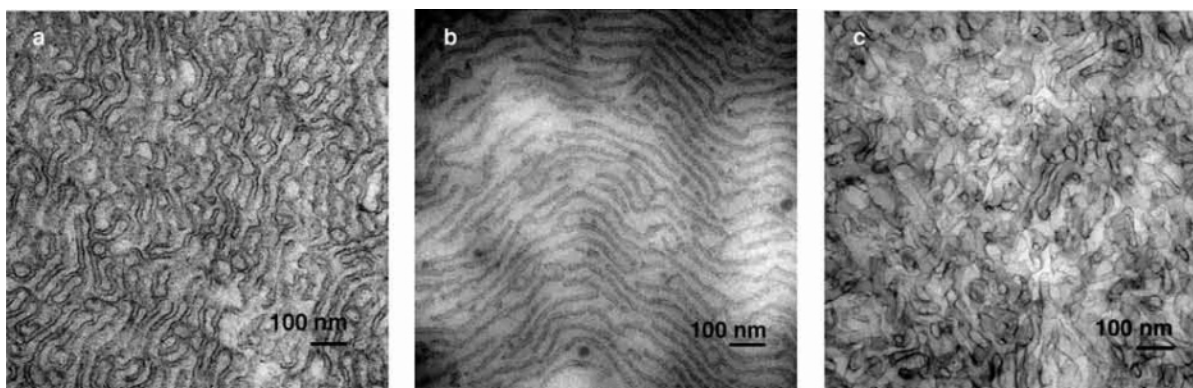


Figure 9. Transmission electron microscope (TEM) images of the A_xBA_x block-graft copolymers [a: $M_n(\text{SEC}) = 147\,000$, $M_w/M_n = 1.24$, A/B = 37/63, $f = 46.1$; b: $M_n(\text{SEC}) = 141\,000$, $M_w/M_n = 1.20$, A/B = 32/68, $f = 10.9$] and the ABA triblock copolymer [c: $M_n(\text{SEC}) = 199\,000$, $M_w/M_n = 1.22$, A/B = 35/65]. Stained by aqueous solution of PTA [12-tungsto(VI)phosphoric acid, *n*-hydrate].

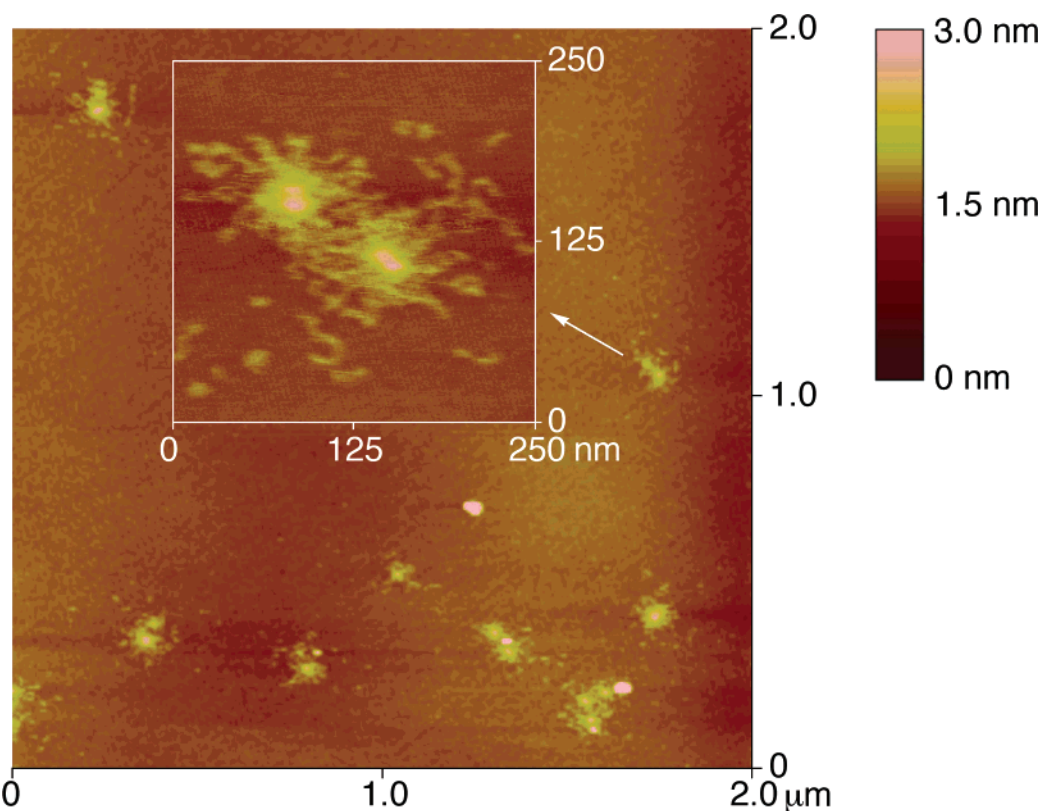


Figure 10. Atomic force microscope (AFM) image of the A_xBA_x block-graft copolymer [$M_n(\text{SEC}) = 791\,000$, $M_w/M_n = 1.27$, A/B = 90/10, $f = 47.5$] obtained with the I₂BI_x multifunctional macroinitiator/Ru(Ind)Cl(PPh₃)₂/Al(acac)₃ in toluene at 80 °C. [MMA]₀ = 8.0 M; [C–X bonds in the macroinitiator]₀ = 10 mM; [Ru(Ind)Cl(PPh₃)₂]₀ = 1.0 mM; [Al(acac)₃]₀ = 40 mM.

(acac)₃ (acac = acetylacetonate; Wako Chemicals, >98%) were used as received. All metal compounds were handled in a glovebox (VAC Nexus) under a moisture- and oxygen-free argon atmosphere (O₂, <1 ppm). Toluene was distilled over sodium benzophenone ketyl and bubbled with dry nitrogen over 15 min just before use. *n*-Bu₃N (as an additive), *n*-hexane, and tetralin (as an internal standards for NMR or gas chromatographic analysis of the monomers) were distilled from calcium hydride before use. 2-Bromoisobutryl bromide (Aldrich, >98%) and 2,2-dichloroacetophenone (Aldrich, >97%) were distilled before use.

Synthesis of Multifunctional Macroinitiator: Ruthenium-Catalyzed Sequential Living Radical Block Copolymerization of DMA and TMSHEMA and One-Pot Transformation to Macroinitiator. All polymerizations were carried out by the syringe technique under dry nitrogen in glass tubes equipped with a three-way stopcock. A typical example for the polymerization of DMA with CHCl₂(COPh)/Ru(Ind)Cl(PPh₃)₂/*n*-Bu₃N is given below. In a 50 mL round-bottomed flask was placed Ru(Ind)Cl(PPh₃)₂ (10 mg,

0.013 mmol), toluene (5.4 mL), tetralin (0.4 mL), DMA (18.8 mL, 64.1 mmol), CHCl₂(COPh) (0.32 mL of 400 mM solution in toluene, 0.128 mmol), and *n*-Bu₃N (0.64 mL of 400 mM solution in toluene, 0.256 mmol) at room temperature. The total volume of reaction mixture was 25.6 mL. The flask was placed in an oil bath kept at 80 °C under vigorous stirring. After the monomer conversion reached 91%, the reaction solution was added TMSHEMA (2.0 mL of 3.23 M solution in toluene, 6.45 mmol). In predetermined intervals, the polymerization was terminated by cooling the reaction mixtures to −78 °C. Monomer conversion was determined by ¹H NMR with tetralin as an internal standard. To the quenched reaction solution was then added toluene (14 mL) and 2-bromoisobutryl bromide (1.6 mL, 13.0 mmol, 2.0 equiv to the trimethylsilyloxy unit) at room temperature under stirring for 24 h. The reaction mixture was precipitated into acetone and isolated by centrifugation. After three times of the precipitation, the precipitate was diluted with toluene and precipitated into methanol. The procedure was repeated three times. The precipitate was then evaporated to dryness

to yield the product, which was subsequently dried overnight in vacuo at room temperature (16.6 g, 97% yield; $M_n = 98\,000$, $M_w/M_n = 1.16$). The polymer was diluted with distilled toluene, and a 2.0 M solution was prepared for the following graft copolymerization.

Synthesis of A_xBA_x Block-Graft Copolymers: Ruthenium-Catalyzed Grafting-From Polymerization of MMA. Graft copolymerizations were also carried out by the syringe technique under dry nitrogen in glass tubes equipped with a three-way stopcock. A typical example for the graft copolymerization of MMA with the multifunctional macroinitiator I_xBI_x with Ru(Ind)Cl(PPh₃)₂/Al(acac)₃ is given below. In a 50 mL round-bottomed flask was placed macroinitiator I_xBI_x (1.2 mL, 0.12 mmol C-Br bonds), toluene (10 mL), hexane (0.5 mL), MMA (0.96 mL, 9.00 mmol), Ru(Ind)Cl(PPh₃)₂ (10 mg, 0.013 mmol), and Al(acac)₃ (0.166 g, 0.51 mmol) at room temperature. The total volume of reaction mixture was 12.8 mL. The flask was placed in an oil bath kept at 80 °C under vigorous stirring. In predetermined intervals, the polymerization was terminated by cooling the reaction mixtures to -78 °C. Monomer conversion was determined by gas chromatography with hexane as an internal standard. The quenched reaction solution was precipitated into methanol and isolated by centrifugation. After three times of the precipitation, the precipitate was evaporated to dryness to yield the product, which was subsequently dried overnight in vacuo at room temperature (0.35 g, 81% yield; $M_n = 126\,000$, $M_w/M_n = 1.23$).

Synthesis of ABA Triblock Copolymers by Ruthenium-Catalyzed Block Copolymerization of MMA. Block copolymerizations were carried out from the poly(DMA) bifunctional initiator. A typical example for the synthesis of poly(DMA) bifunctional macroinitiator with CHCl₂(COPh)/Ru(Ind)Cl(PPh₃)₂/*n*-Bu₃N is given below. In a 50 mL round-bottomed flask were placed Ru(Ind)Cl(PPh₃)₂ (12.7 mg, 0.017 mmol), toluene (7.0 mL), tetralin (0.6 mL), DMA (23.4 mL, 79.8 mmol), CHCl₂(COPh) (0.1 mL of 800 mM solution in toluene, 0.080 mmol), and *n*-Bu₃N (0.8 mL of 400 mM solution in toluene, 0.320 mmol) at room temperature. The total volume of reaction mixture was 32.0 mL. The flask was placed in an oil bath kept at 80 °C under vigorous stirring. In predetermined intervals, the polymerization was terminated at ~50% conversion by cooling the reaction mixtures to -78 °C. Monomer conversion was determined by ¹H NMR with tetralin as an internal standard. The reaction mixture was precipitated into acetone and isolated by centrifugation. After three times of the precipitation, the precipitate was diluted with toluene and precipitated into methanol. The procedure was repeated three times. The precipitate was then evaporated to dryness to yield the product, which was subsequently dried overnight in vacuo at room temperature (12.5 g, 94% yield; $M_n = 116\,000$, $M_w/M_n = 1.21$). The polymer was diluted with distilled toluene, and a 2.0 M solution was prepared for the following block copolymerization. A typical example for the block copolymerization of MMA on the poly(DMA) bifunctional macroinitiator with Ru(Ind)Cl(PPh₃)₂/Al(acac)₃ is given below. In a 50 mL round-bottomed flask was placed poly(DMA) bifunctional macroinitiator (7.1 mL, 0.0276 mmol C-Cl bond), *n*-hexane (0.5 mL), MMA (6.0 mL, 55.7 mmol), Ru(Ind)Cl(PPh₃)₂ (10.7 mg, 0.014 mmol), and Al(acac)₃ (0.179 g, 0.55 mmol) at room temperature. The total volume of reaction mixture was 13.8 mL. The flask was placed in an oil bath kept at 80 °C under vigorous stirring. In predetermined intervals, the polymerization was terminated by cooling the reaction mixtures to -78 °C. Monomer conversion was determined by gas chromatography with hexane as an internal standard. The quenched reaction solution was precipitated into methanol and isolated by centrifugation. After three times of the precipitation, the precipitate was evaporated to dryness to yield the product, which was subsequently dried overnight in vacuo at room temperature (2.54 g, 90% yield; $M_n = 189\,000$, $M_w/M_n = 1.18$).

Measurements. The ¹H NMR spectra were recorded on a Varian Gemini 2000 spectrometer (400 MHz). The number-average molecular weights (M_n) and molecular weight distributions (MWDs: M_w/M_n) of the polymers were measured by size exclusion

chromatography (SEC) using THF at a flow rate 1.0 mL/min at 40 °C on two polystyrene gel columns (both Shodex KF-805L) that were connected to a JASCO PU-980 precision pump and a JASCO RI-930 detector. The molecular weight was calibrated against seven standard poly(methyl methacrylate) samples ($M_n = 1990$ – $6\,590\,000$) or eight standard polystyrene samples ($M_n = 526$ – $900\,000$). The monomer conversions were determined from the concentration of the residual monomer measured by gas chromatography using hexane or tetralin as the internal standard. The absolute weight-average molecular weight (M_w) of the polymers was determined by multiangle laser light scattering in tetrahydrofuran (THF) at 40 °C on a Wyatt Technology DAWN DSP photometer ($\lambda = 633$ nm). The refractive index increment (dn/dc) was measured in THF at 25 °C on a Wyatt Optilab rEX refractometer ($\lambda = 633$ nm); the dn/dc values were 0.072–0.127 mL/g for the A_xBA_x block-graft copolymers. Sample films for dynamic tensile viscoelasticity and transmission electron microscopy (TEM) were prepared by hot-press molding of the copolymers at 230 °C. Dynamic tensile storage (E') and loss (E'') moduli and $\tan \delta$ ($= E''/E'$) were measured on a UBM Rheogel-E4000 spectrometer, operating at 11 Hz frequency (heating rate: 10 °C/min). For TEM, the ultrathin sections of the sample were cut on a Leica Ultracut FCS microtome at -100 °C (ca. 70 nm) and collected on mesh copper grids. The thin sections were stained with an aqueous solution of PTA [12-tungsto(VI)phosphoric acid, *n*-hydrate] containing small amounts of benzyl alcohol, washed with water, and then vacuum-dried at room temperature. Micrographs were obtained by a transmission electron microscope H-7100 FA (Hitachi, Ltd.) equipped with a CCD digital camera (AMT, Ltd.) operated at an acceleration voltage of 100 kV. Atomic force microscopy (AFM) observations were performed on a Nanoscope IIIa microscope (Digital Instruments, Santa Barbara, CA) in air using standard silicon tips (NCH-10V) in the tapping mode. All the images were collected with the maximum available number of pixels (512) in each direction (2 μ m or 500 nm).

Acknowledgment. This work was supported in part by the 21st Century COE Program "Nature-Guided Materials Processing", the Ogasawara Foundation for the Promotion of Science & Engineering, Iketani Science and Technology Foundation, Izumi Science and Technology Foundation, and the Project to Develop "Innovative Seeds" from Japan Science and Technology Agency. H.J. is grateful to the New Energy and Industrial Technology Development Organization (NEDO) for supporting this study through a Japanese National Project "Nano Structure Polymer Project" by the Ministry of Economy, Trade and Industry. H.J. also thanks the Japan Society for the Promotion of Science for partial support of this research through a Grain-in-Aid for Scientific Research (C) No. 18550194. We thank Mr. Sousuke Ohsawa, Prof. Eiji Yashima (Nagoya University and Yashima Super-structured Helix Project, Exploratory Research for Advanced Technology: ERATO) and Dr. Jiro Kumaki (Yashima Super-structured Helix Project, Exploratory Research for Advanced Technology: ERATO) for technical support and useful suggestions on AFM and Messrs Isamu Okamoto and Atsuhiko Nakahara (Kuraray Co. Ltd., Tsukuba Research Laboratories) for the measurements of tensile viscoelasticity.

References and Notes

- (1) (a) Morton, M. *Anionic Polymerization: Principles and Practice*; Academic Press: New York, 1983; pp 221–232. (b) Kennedy, J. P.; Ivan, B. *Designed Polymers by Carbocationic Macromolecular Engineering: Theory and Practice*; Hanser Publishers: Munich, 1992; p 96. (c) Sawamoto, M.; Kamigaito, M. In *New Methods of Polymer Synthesis*; Ebdon, J. R., Eastmond, G. C., Eds.; Blackie: Glasgow, UK, 1995; Vol. 2, pp 37–68.
- (2) (a) Georges, M. K.; Veregin, R. P. N.; Kazmaier, P. M.; Hamer, G. K. *Macromolecules* **1993**, *26*, 2987–2988. (b) Georges, M. K.;

- Veregin, R. P. N.; Kazmaier, P. M.; Hamer, G. K. *Trends Polym. Sci.* **1994**, *2*, 66–72.
- (3) (a) Hawker, C. J. *J. Am. Chem. Soc.* **1994**, *116*, 11185–11186. (b) Hawker, C. J.; Bosman, A. W.; Harth, E. *Chem. Rev.* **2001**, *101*, 3661–3688.
- (4) (a) Kato, M.; Kamigaito, M.; Sawamoto, M.; Higashimura, T. *Macromolecules* **1995**, *28*, 1721–1723. (b) Kamigaito, M.; Ando, T.; Sawamoto, M. *Chem. Rev.* **2001**, *101*, 3689–3745.
- (5) Kamigaito, M.; Ando, T.; Sawamoto, M. *Chem. Rec.* **2004**, *4*, 159–175.
- (6) (a) Wang, J.-S.; Matyjaszewski, K. *J. Am. Chem. Soc.* **1995**, *117*, 5614–5615. (b) Matyjaszewski, K.; Xia, J. *Chem. Rev.* **2001**, *101*, 2921–2990.
- (7) Percec, V.; Barboiu, B. *Macromolecules* **1995**, *28*, 7970–7972.
- (8) Granel, C.; Dubois, P.; Jérôme, R.; Teyssié, P. *Macromolecules* **1996**, *29*, 8576–8582.
- (9) Haddleton, D. M.; Jasieczek, C. B.; Hannon, M. J.; Shooter, A. J. *Macromolecules* **1997**, *30*, 2190–2193.
- (10) (a) Chiefari, J.; Chong, Y. K.; Ercole, F.; Krstina, J. Jeffery, K.; Tam, P. T. Le.; Mayadunne, R. T. A.; Meijs, G. F.; Moad, C. L.; Moad, G.; Rizzardo, E.; Thang, S. H. *Macromolecules* **1998**, *31*, 5559–5562. (b) Chong, Y. K.; Kristina, J.; Tam, P. T. Le.; Moad, G.; Postma, A.; Rizzardo, E.; Thang, S. H. *Macromolecules* **2003**, *36*, 2256–2272. (c) Chiefari, J.; Mayadunne, R. T. A.; Moad, C. L.; Moad, G.; Rizzardo, E.; Postma, A.; Skidmoe, M. A.; Thang, S. H. *Macromolecules* **2003**, *36*, 2273–2283.
- (11) Destarac, M.; Bzducha, W.; Taton, D.; Gauthier-Gillaizeau, I.; Zard, S. Z. *Macromol. Rapid Commun.* **2002**, *23*, 1049–1054.
- (12) (a) Yamago, S.; Iida, K.; Yoshida, J. *J. Am. Chem. Soc.* **2002**, *124*, 2874–2875. (b) Yamago, S.; Ray, B.; Iida, K.; Yoshida, J.; Tada, T.; Yoshizawa, K.; Kwak, Y.; Goto, A.; Fukuda, T. *J. Am. Chem. Soc.* **2004**, *126*, 13908–13909.
- (13) Wayland, B. B.; Poszmik, G.; Mukerjee, S. L.; Fryd, M. *J. Am. Chem. Soc.* **1994**, *116*, 7943–7944.
- (14) Debuigne, A.; Caille, J.-R.; Jérôme, R. *Angew. Chem., Int. Ed.* **2005**, *44*, 1101–1104.
- (15) Kotani, Y.; Kato, M.; Kamigaito, M.; Sawamoto, M. *Macromolecules* **1996**, *29*, 6979–6982.
- (16) Miura, Y.; Satoh, K.; Kamigaito, M.; Okamoto, Y. *Polym. J.* **2006**, *38*, 930–939.
- (17) (a) Ueda, J.; Matsuyama, M.; Kamigaito, M.; Sawamoto, M. *Macromolecules* **1998**, *31*, 557–562. (b) Ueda, J.; Kamigaito, M.; Sawamoto, M. *Macromolecules* **1998**, *31*, 6762–6768. (c) Baek, K.-Y.; Kamigaito, M.; Sawamoto, M. *Macromolecules* **2001**, *34*, 215–221.
- (18) Holden, G.; Kricheldorf, H. R.; Quirk, R. P. *Thermoplastic Elastomers*, 3rd ed.; Hanser Publishers: Munich, 2004.
- (19) (a) Moineau, G.; Minet, M.; Teyssié, Ph.; Jérôme, R. *Macromolecules* **1999**, *32*, 8277–8282. (b) Tong, J. D.; Moineau, G.; Leclère, Ph.; Bredas, J. L.; Lazzaroni, R.; Jérôme, R. *Macromolecules* **2000**, *33*, 470–479.
- (20) Matyjaszewski, K.; Shipp, D. A.; McMurtry, G. P.; Gaynor, S. G.; Pakula, T. *J. Polym. Sci., Part A: Polym. Chem.* **2000**, *38*, 2023–2031.
- (21) For reviews, see: (a) Davis, K. A.; Matyjaszewski, K. *Adv. Polym. Sci.* **2002**, *159*, 107–152. (b) Börner, H.; Matyjaszewski, K. *Macromol. Symp.* **2002**, *177*, 1–15. (c) Bhattacharya, A.; Misra, B. N. *Prog. Polym. Sci.* **2004**, *29*, 767–814.
- (22) (a) Beers, K. L.; Gaynor, S. G.; Matyjaszewski, K.; Sheiko, S. S.; Möller, M. *Macromolecules* **1998**, *31*, 9413–9415. (b) Börner, H. G.; Beers, K. L.; Matyjaszewski, K.; Sheiko, S. S.; Möller, M. *Macromolecules* **2001**, *34*, 4375–4383. (c) Börner, H. G.; Duran, D.; Matyjaszewski, K.; da Silva, M.; Sheiko, S. S. *Macromolecules* **2002**, *35*, 3387–3394. (d) Qin, S.; Matyjaszewski, K.; Xu, H.; Sheiko, S. S. *Macromolecules* **2003**, *36*, 605–612. (e) Lord, S. J.; Sheiko, S. S.; LaRue, I.; Lee, H.-I.; Matyjaszewski, K. *Macromolecules* **2004**, *37*, 4235–4240. (f) Lee, H.; Matyjaszewski, K.; Yu, S.; Sheiko, S. S. *Macromolecules* **2005**, *38*, 8264–8271.
- (23) Sumerlin, B. S.; Neugebauer, D.; Matyjaszewski, K. *Macromolecules* **2005**, *38*, 702–708.
- (24) (a) Cheng, G.; Böker, A.; Zhang, M.; Krausch, G.; Müller, A. H. E. *Macromolecules* **2001**, *34*, 6883–6888. (b) Mori, H.; Müller, A. H. E. *Prog. Polym. Sci.* **2003**, *28*, 1403–1439. (c) Cai, Y.; Hartenstein, M.; Müller, A. H. E. *Macromolecules* **2004**, *37*, 7484–7490.
- (25) Ma, Y. H.; Cao, T.; Webber, S. E. *Macromolecules* **1998**, *31*, 1773–1778.
- (26) Chen, G.; Hoffman, A. S. *Nature (London)* **1995**, *373*, 49–52.
- (27) Shibamura, T.; Aoki, T.; Sanui, K.; Ogata, N.; Kikuchi, A.; Sakurai, Y.; Okano, T. *Macromolecules* **2000**, *33*, 444–450.
- (28) Li, C.; Gunari, N.; Fischer, K.; Janshoff, A.; Schmidt, M. *Angew. Chem., Int. Ed.* **2004**, *43*, 1101–1104.
- (29) Janata, M.; Lochmann, L.; Brus, J.; Holler, P.; Tuzar, Z.; Kratochvíl, P.; Schmitt, B.; Radke, W.; Müller, A. H. E. *Macromolecules* **1997**, *30*, 7370–7374.
- (30) (a) Floudas, G.; Hadjichristidis, N.; Iatrou, H.; Avgeropoulos, A.; Pakula, T. *Macromolecules* **1998**, *31*, 6943–6950. (b) Houli, S.; Iatrou, H.; Hadjichristidis, N.; Vlassopoulos, D. *Macromolecules* **2002**, *35*, 6592–6597.
- (31) Knauss, D. M.; Huang, T. *Macromolecules* **2002**, *35*, 2055–2062.
- (32) Huang, T.; Knauss, D. M. *Polym. Bull. (Berlin)* **2002**, *49*, 143–150. (b) Huang, T.; Knauss, D. M. *Macromol. Symp.* **2004**, *215*, 81–93.
- (33) Knauss, D. M.; Huang, T. *Macromolecules* **2003**, *36*, 6036–6042.
- (34) Ruckenstein, E.; Zhang, H. *Macromolecules* **1998**, *31*, 2977–2982. (b) Zhang, H.; Ruckenstein, E. *Macromolecules* **1998**, *31*, 4753–4759.
- (35) Lai, M.-K.; Wang, J.-Y.; Tsiang, R. C.-C. *Polymer* **2005**, *46*, 2558–2566.
- (36) Pan, Q.; Liu, S.; Xie, J.; Jiang, M. *J. Polym. Sci., Part A: Polym. Chem.* **1999**, *37*, 2699–2702.
- (37) Ning, F.; Jiang, M.; Mu, M.; Duan, H.; Xie, J. *J. Polym. Sci., Part A: Polym. Chem.* **2002**, *40*, 1253–1266.
- (38) Truelsen, J. H.; Kops, J.; Batsberg, W. *Macromol. Rapid Commun.* **2000**, *21*, 98–102.
- (39) (a) Truelsen, J. H.; Kops, J.; Batsberg, W.; Armes, S. P. *Macromol. Chem. Phys.* **2002**, *203*, 2124–2131. (b) Truelsen, J. H.; Kops, J.; Batsberg, W.; Armes, S. P. *Polym. Bull. (Berlin)* **2002**, *49*, 235–242.
- (40) Lecolley, F.; Waterson, C.; Carmichael, A. J.; Mantovani, G.; Harrisson, S.; Chappell, H.; Limer, A.; Williams, P.; Ohno, K.; Haddleton, D. M. *J. Mater. Chem.* **2003**, *13*, 2689–2695.
- (41) Ohno, S.; Matyjaszewski, K. *J. Polym. Sci., Part A: Polym. Chem.* **2006**, *44*, 5454–5467.
- (42) Fuji, Y.; Watanabe, K.; Beak, K.-Y.; Ando, T.; Kamigaito, M.; Sawamoto, M. *J. Polym. Sci., Part A: Polym. Chem.* **2002**, *40*, 2055–2065.
- (43) Takahashi, H.; Ando, T.; Kamigaito, M.; Sawamoto, M. *Macromolecules* **1999**, *32*, 3820–3823.
- (44) Podzimek, S.; Vlcek, T. *J. Appl. Polym. Sci.* **2001**, *82*, 454–460.
- (45) Vankan, R.; Fayt, R.; Jérôme, R.; Teyssié, Ph. *Polym. Eng. Sci.* **1996**, *36*, 1675–1684.
- (46) (a) Fox, T. G.; Flory, P. J. *J. Appl. Phys.* **1950**, *21*, 581–591. (b) Fox, T. G.; Flory, P. J. *J. Polym. Sci.* **1954**, *14*, 315–319.
- (47) Turner, D. T. *Polymer* **1978**, *19*, 789–796.
- (48) Bates, F. S.; Fredrickson, G. H. *Annu. Rev. Phys. Chem.* **1990**, *41*, 525–557.
- (49) Kitayama, T.; Ogawa, M.; Kawauchi, T. *Polymer* **2003**, *44*, 5201–5207.
- (50) Matyjaszewski, K.; Qin, S.; Boyce, J. R.; Shirvnyants, D.; Sheiko, S. S. *Macromolecules* **2003**, *36*, 1843–1849.